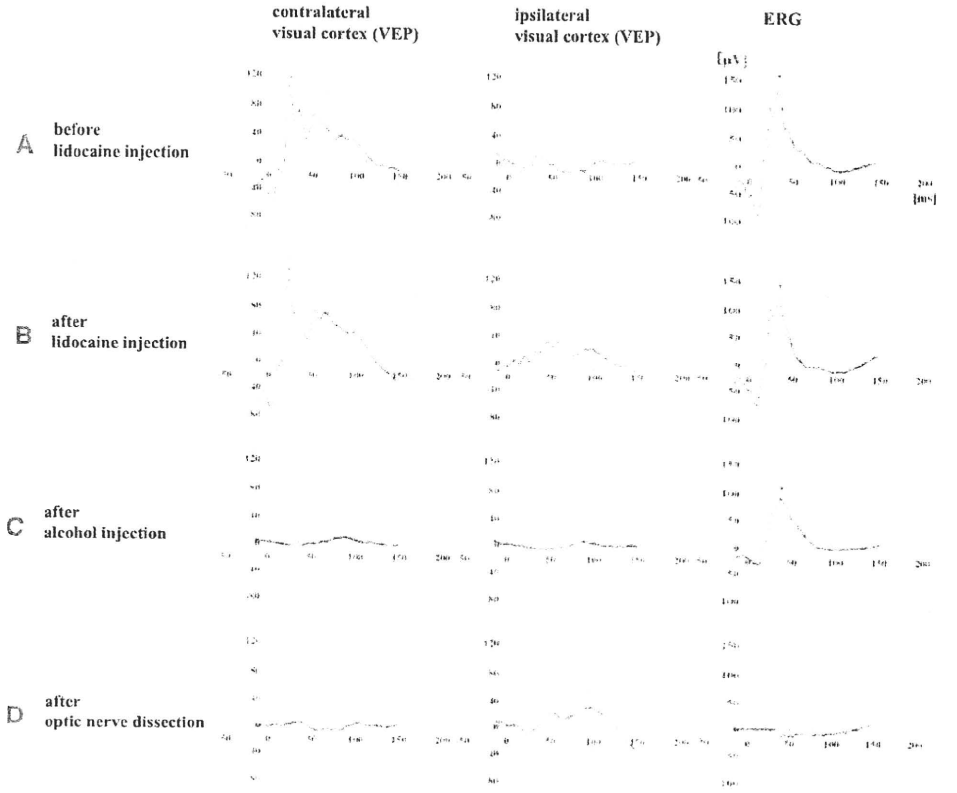

Figure 2A–D. Preliminary experimental series: cortical visual evoked potential (*VEP*) and retinal electroretinogram (*ERG*) responses to light in unimplanted rabbits: **A** before and **B** after retrobulbar injection of 4% lidocaine; **C** after retrobulbar injection of 99% alcohol, and **D** after transecting the optic nerve. A strong positive component at approximately 20 ms was observed in the VEPs from contralateral visual cortex (*arrow*); recordings from the ipsilateral cortex were within noise level. VEPs of similar shape were reported before.[24,31] Retrobulbar injection of 4% lidocaine did not alter this cortical response, corresponding to the clinical observation that retrobulbar injection of local anesthetic sometimes cannot eliminate the patient's light sensation during ocular surgery. After 99% alcohol injection, the contralateral VEP response disappeared. Transection of the optic nerve extinguished ipsi- and contralateral responses. The b wave of the corneal ERG was unaltered after retrobulbar injection of 4% lidocaine, but decreased somewhat after injection of 99% alcohol. Transection of the optic nerve completely extinguished any ERG response. Flash intensity: . 0.2 $cd^{*}s/m^{2}$; . 2.0 $cd^{*}s/m^{2}$; ——, 20.0 $cd^{*}s/m^{2}$.

Preliminary Series

To discriminate biological responses from the small and artifact-laden responses following electrical stimulation, we characterized normal retinal and cortical responses from animals without subretinal implantation in a preliminary series in two rabbits. VEPs and ERGs were recorded before and after the following two experimental conditions in two rabbits: (1) retrobulbar injection of either 1 ml of 4% lidocaine or 1 ml of 99% ethyl alcohol to exclusively block optic nerve transduction while sparing retinal responses, and (2) transection of the optic nerve to disrupt retinal as well as cortical responses. Results are shown in Fig. 2.

Preparation for Histology

The posterior globe was immersed in 10% formaldehyde. Then, tissue blocs corresponding to the area of the implantation channel and the area overlying the foil strip were dissected and embedded in paraffin for light microscopy, and then stained with H&E. For immunohistochemistry, 6-μm sections were stained with a rod photoreceptor cell specific marker against the N-terminal region of rhodopsin (mouse hybridoma monoclonal antibody Rho 4D2; generously provided by Professor R. S. Molday, Department of Biochemistry and Molecular Biology, Faculty of Medicine, University of British Columbia, Vancouvar, Canada). In brief, deparaffinized tissue sections were washed for 5 min in phosphate-buffered saline (PBS), blocked for 30 min in PBS plus 10% serum plus 1% bovine serum albumin (BSA), then incubated with the primary antibody overnight, dilution 1:60. After three washings in PBS/BSA for 5 min each time, incubation with a secondary antibody for 1 h (fluorescein isothiocyanate-conjugated sheep anti-mouse Ab; 1:50, F6257-1ML; Sigma, St. Louis, MO, USA), the specimens were rinsed again, equilibrated (MP equ-buffer) and examined under a fluorescence microscope (Leica DMBR, Leica, Wetzlar, Germany).

Jpn J Ophthalmol
Vol 54: 467–475, 2010

Results

Transchoroidal Surgery

Transchoroidal surgery was performed uneventfully in all four rabbits through the same subretinal implantation channel. The implant was successfully inserted into the subretinal space in all 16 procedures in all animals. No significant choroidal bleeding occurred at the entry site. In one eye, retinal perforation occurred at the site of the choroidal incision during one surgical session. In that case, the protruding vitreous was pushed back by an additional flexible plastic foil. Thereafter, the subretinal implantation was successful.

Rabbits 1 and 2

Rabbits 1 and 2 were implanted with a subretinal MPDA prototype (diameter, 2.5 mm; thickness, 50 μm) as described before,[26] and the prototype was bonded onto the tip of a polyimide foil strip (thickness, 30 μm; width, 2.7 mm; length, 20 mm; Fig. 3A). The device was explanted 4 weeks later. The animals were euthanized 2 weeks after explantation for histological assessment of the retina. Explantation revealed conjunctival scarring and attachment of the conjunctiva to the underlying scleral flap. The implant could be removed uninjured without encountering bleedings or retinal complications. The retina remained attached both during implantation of the device and after removal. At all examination dates the outer aspect of the eyes remained well preserved, the conjunctiva was closed, and no signs of atrophy, infection, or wound dehiscence were detectable. Details are shown in Fig. 4A–C and in Table 1. Histology showed a well-preserved neurosensory retinal architecture across the implantation (not shown).

Rabbit 3

Rabbit 3 underwent two implantations and two explantations and functional evaluation. In the primary surgical session, it received the same implant as rabbits 1 and 2, which was exchanged after 13 months for an electrically functioning foil strip (Fig. 3B) for subretinal electrical stimulation and to record retinal and cortical potentials. Between the two surgeries, the outer aspect of the operated eye remained without any signs of infection, atrophy, or wound dehiscence. Funduscopy revealed stable positioning of the subretinal implant in the eye. No retinal detachment or proliferative reaction, but some retinal pigment epithelium (RPE) degeneration was observable in the region around the implant. In the second surgical session the degree of conjunctival/scleral scarring was not remarkably higher than in rabbits 1 and 2 (after 4 weeks). The stimulation foil was then introduced after removal of the first implant through the previous implantation channel and advanced some millimeters further to ensure its position under untouched retinal regions. Transchoroidal access to the subretinal space was uneventful, as was water-tight wound closure of the scleral flap.

Comparison of the b-wave amplitudes of the ERGs showed a reduction by approximately 20% in the implanted versus the unimplanted eye, whereas VEPs from the implanted and the unimplanted eyes were identical (in agreement with rabbit 4, see Fig. 5). VEPs from the contralateral visual cortex disappeared after alcohol injection. ERGs did not change in shape between before and after alcohol injection, as was to be expected from the preliminary experiments, but disappeared after transection of the optic nerve.

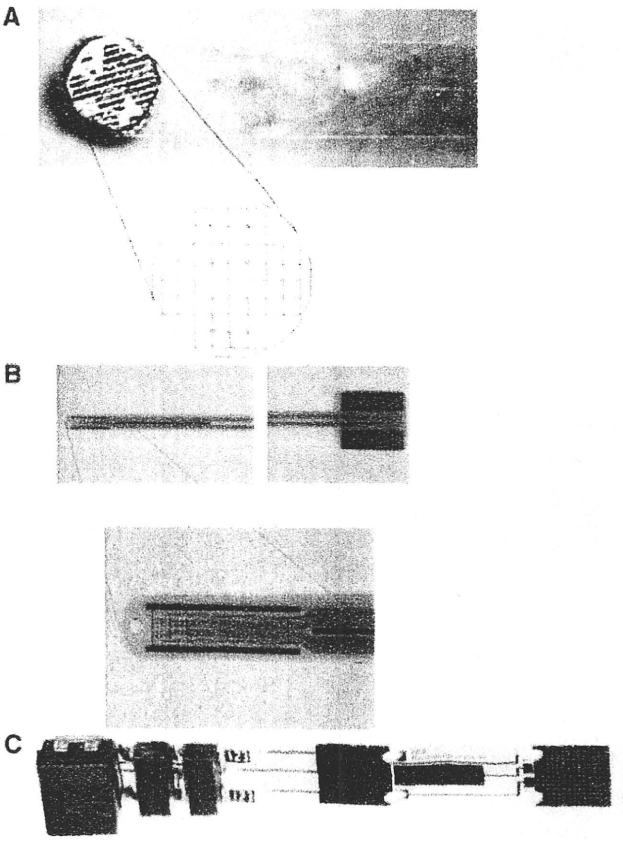

Figure 3A–C. Photographs of the subretinal implants used in this study. **A** The implant of rabbit 1 and 2 consisted of a microphotodiode-array which was glued onto a polyimide foil (2 mm wide, ca. 30 μm thick). The array comprised 12 inactive electrodes each with 4 surrounding microphotodiodes (50 μm thickness, diameter ca. 2 mm; enlarged photo). **B** The final implant was used for subretinal electrical stimulation in the final surgery in rabbits 3 and 4. The polyimide foil strip (thickness 12 μm, width 2.4 mm, length 48.0 mm) with 32 gold connection lanes terminating in a 5 × 6 array with 32 titanium nitride electrodes (30 active electrodes 50 μm in diameter and two larger reference electrodes) at the end of the strip as has been described before.[34] Each electrode can be connected to an external stimulus generator. **C** The complex implant used in rabbit 4 with extraocular parts (thickness up to 2 mm, width 3 mm, length 22 mm). The stimulating and photodiode array is on the right, the infrared-sensitive energy-receiving photodiode is in the center, and the electronic units are on the left. It stayed in place for 5 weeks and was the second implant used in this rabbit.

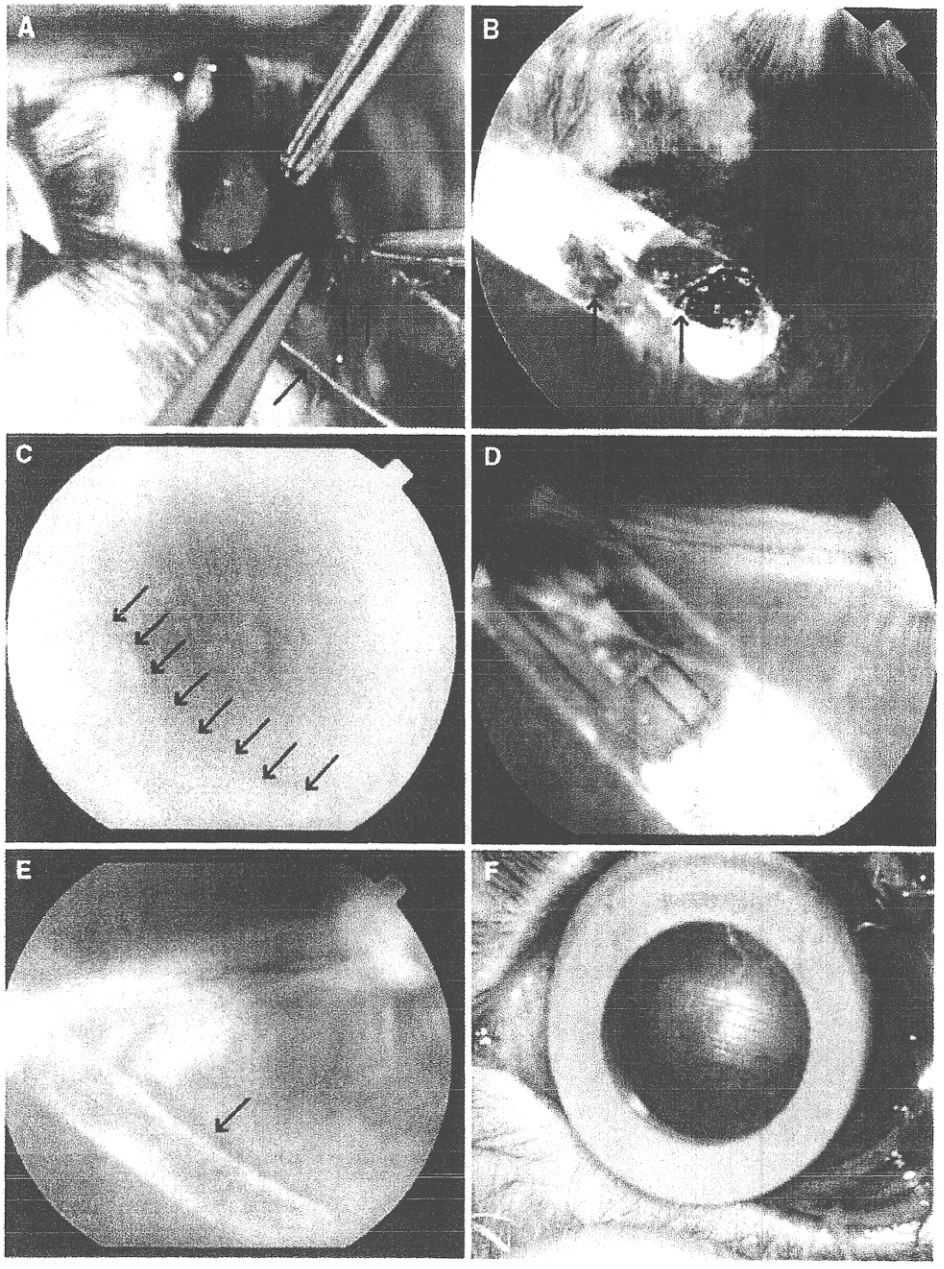

Figure 4A–F. Different photographic aspects of rabbits 1 and 4. **A** Transchoroidal surgery of rabbit 1. Along a guiding foil (single arrow) the polyimide foil strip with a microphotodiode array on its tip (double arrow) was inserted into the subretinal space. **B** Fundus of rabbit 1 *four* weeks postoperatively with the foil in the subretinal space. Neither inflammatory changes nor retinal detachment were found, but two necrotic retinal holes (arrows) overlying the foil *caused by* lack of nutrition from the retinal pigment epithelium were observed. **C** Fundus of rabbit 1 *two* weeks after explantation. Retinal pigment epithelium alteration was found in the area of the previous explantation/implantation channel (arrows). **D** Fundus of rabbit 4 after second implantation (out of *four*). A functioning device was reimplanted transchoroidally through the previous implantation channel and placed subretinally. **E** Fundus of rabbit 4 eight weeks after the third implantation. The subretinally implanted foil (arrow) was stable in position. Besides some depigmentation and choroidal scarring, the retina showed no obvious damage. **F** Fundus of rabbit 4 after the fourth and final implantation, which was successfully performed through the same subretinal implantation channel; a functioning 32-channel oil for acute electrical stimulation was placed subretinally

Retinal susceptibility to electrical stimulation was proven by recording eERGs with a reproducible positivity of approximately 20 μV and a latency of 20 ms (Fig. 6B). The response was stable after optic nerve block, but disappeared after the animal was euthanized. Electrically evoked cortical potentials from the contralateral cortex were also successfully recorded (Fig. 6A). The surgical situation did not allow transection of the optic nerve without endangering the stability of the subretinal foil connected to the stimulus generator.

Histological results are shown in Fig. 7A, B. Areas untouched by the subretinal implant in the posterior pole were histologically unaltered (not shown).

Rabbit 4

Following the good results of the previous experiments, rabbit 4 underwent four transchoroidal implantations and four explantations. In the first surgery the same device as in the previous three rabbits was implanted for 8 weeks. It was

Jpn J Ophthalmol
Vol 54: 467–475, 2010

Table 1. Summary of experiments

Rabbit no.	Surgery	Time to next surgery	Implant size max. thickness × width × length (mm)	Type of function testing	Figures
1 and 2	1: Implantation	4 weeks	0.08 × 2 × 15	VEP, ERG	Operation: 4A
	2: Explantation	2 weeks			Fundus: 4B,C
	3: Euthanized	Function testing			Electrophysiology: 2
3	1: Implantation	13 months	0.08 × 2 × 15	VEP, ERG, eERG, eECP	Histology: 7A,B
	2: Explantation, reimplantation, euthanized	Acute stimulation experiment	0.012 × 48 × 2.4 (Fig. 3B)		Electrophysiology: 6A
4	1: Implantation	8 weeks	0.08 × 2 × 15	VEP, ERG, eERG, eECP	Fundus: 4D,E,F
	2: Explantation, reimplantation	5 weeks	2 × 3 × 22 (Fig. 3A)		Histology: 7C,D
	3: Explantation, reimplantation	7 months	0.03 × 2 × 17		Electrophysiology: 5,6B
	4: Explantation, reimplantation, euthanized	Acute stimulation experiment	0.012 × 2.4 × 48 (Fig. 3B)		

VEP, visually evoked potential; ERG, electroretinogram to light stimulation; eERG, electroretinograms to subretinal electrical stimulation; eECP, electrically evoked cortical potential.

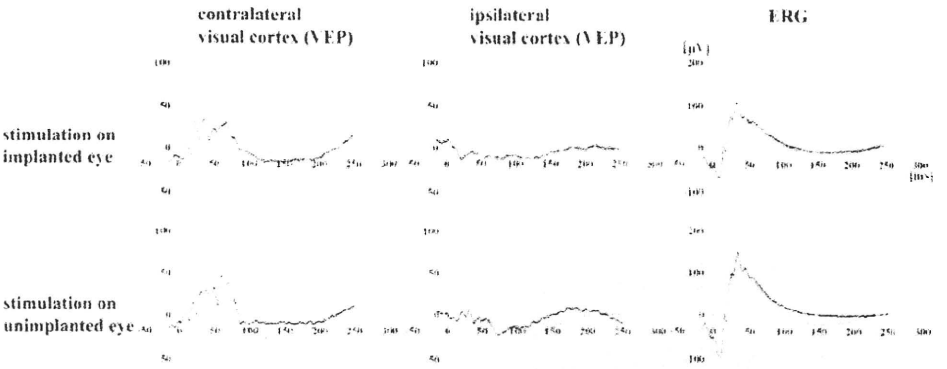

Figure 5. Cortical (VEP) and retinal (ERG) responses of the implanted and unimplanted eye in rabbit 4 immediately before the fourth and final implantation after 10 months. A strong positive component at approximately 50 ms was observed in the VEPs from contralateral visual cortex. While b-wave amplitudes in the ERG were reduced by approximately 20% in the implanted eye, similar VEPs from both eyes were recorded with full-field flash stimulation from both eyes, demonstrating good preservation of the retina after multiple implantations and explantations. Flash intensity: , 0.2 cd·s/m^2; , 2.0 cd·s/m^2; ——, 20.0 cd·s/m^2.

exchanged in the second surgery for a larger, more complex implant with extraocular parts (Fig. 3C), which stayed subretinally for 5 weeks (Fig. 4D). In the third surgery it was exchanged for a polyimide foil strip with a large permanent extraocular part (thickness, approximately 0.03 mm; width, 2 mm; length, 17 mm; Fig. 4E), which stayed subretinally for 7 months. In the fourth and final surgery an electrically functioning polyimide foil strip (Fig. 3B) was implanted for recording of retinal and cortical potentials after subretinal electrical stimulation (Fig. 4F).

As in the previous experiments, the eye was well preserved during the entire period of 10 months (Fig. 4D–F). The retina remained attached and no signs of either inflammation or adverse reactions were noticed on either external inspection or funduscopy. The retina at the region of the implant on the posterior pole, however, showed several atrophic holes, and in some areas a fibrous tissue reaction was observed. Despite tissue scarring as described above, we found it feasible in all surgeries to expose the implant, prepare the scleral flap, open it, and access the subretinal space transchoroidally to explant the old device and implant a new one. No complications occurred during any surgery. Entry sites of the sclera and the choroid were in such a state that access was possible without further incision.

From the implanted and the unimplanted eye, identical VEPs were recorded at the beginning of the final acute implantation as well as immediately after completing the surgery. ERG amplitudes at the time were reduced by approximately 20% (Fig. 5). VEPs and ERGs showed analogous behavior to those in rabbit 3 after alcohol injection. Transection of the optic nerve was possible in this animal and led to extinguished ERGs and VEPs.

eERGs showed analogous results to those in rabbit 3, proving intact retinal function and susceptibility to subretinal electrical stimulation after multiple surgeries (Fig. 6B). No discernible response was obtained, however, in the eECP recordings in this rabbit. eERGs and eECPs were rerecorded after euthanizing the animal and extinction of the eERG was demonstrated (Fig. 6B).

Histology in rabbit 4 is shown in Fig. 7C, D.

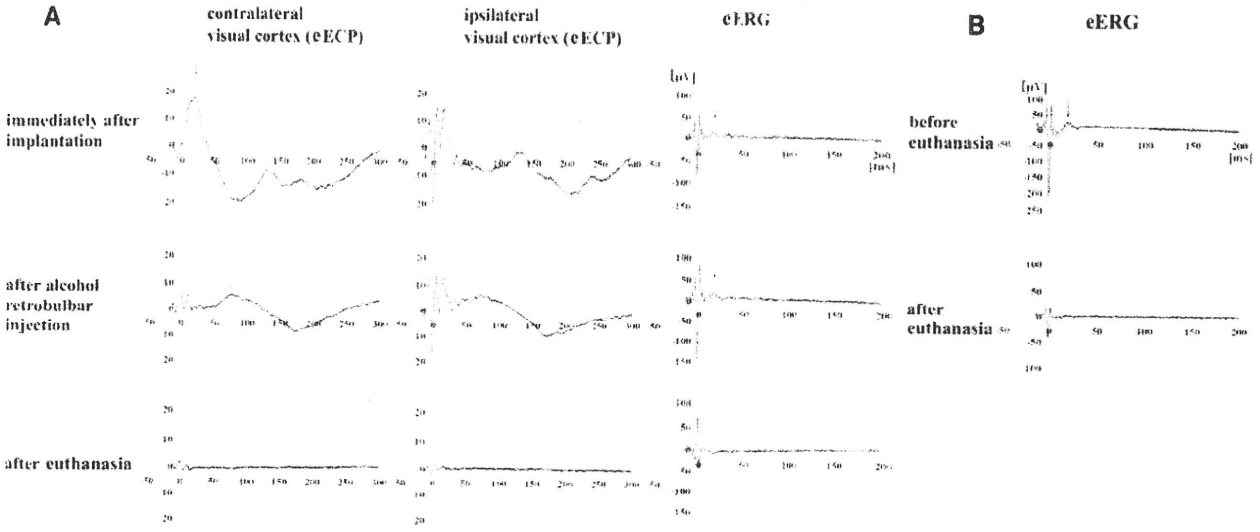

Figure 6A, B. Electrically evoked cortical potential (eECP) and retinal responses (eERG) following subretinal electrical stimulation in rabbits 3 and 4. *A* eECPs in rabbit 3 with a positive component (arrow) at approximately 20 ms in the recordings from the contralateral visual cortex immediately after the final implantation. After 99% alcohol injection into the retrobulbar space, the response disappeared. Recordings from the ipsilateral cortex remained within noise level. The positive component (arrow) in the eERG at approximately 15 ms observed in the recordings immediately after implantation as well as after optic nerve block disappeared after the animal *was euthanized*. Transection of the optic nerve could not be performed as planned without endangering the stability of the subretinal foil due to the surgical situation. *B* eERG recordings in rabbit 4 show a clear positivity of approximately 20 µV with a latency of 20 ms. In the *euthanized* animal (lower trace) no such response was observed. Stimulation strength: , 2 V; , 2.5 V; ——, 3.0 V.

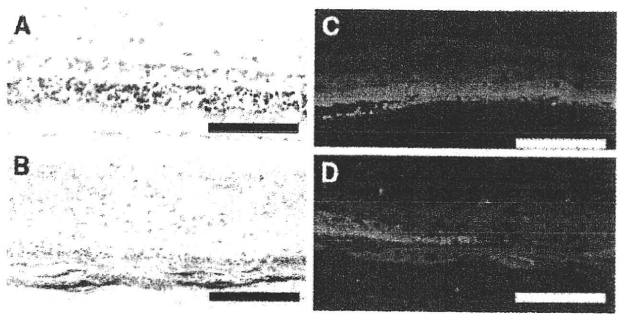

Figure 7A–D. Histological preparation of retinas. H&E stained retinal sections are shown *on* the left, *and* immunohistochemical rhodopsin-stained sections *on* the right (scale bars = 50 µm), immediately after repeated implantation/explantation surgeries and subretinal electrical stimulation in rabbits 3 (A, B) and 4 (C, D). **A** The retina shows *a* small degree of disorganization and retinal edema in the area overlying the stimulation foil after short-term stimulation in the final acute experiment. **B** The immunohistochemical staining for rhodopsin shows evenly distributed, well-preserved rhodopsin in all areas over the electrode foil even after repeated subretinal electrical stimulation. **C** H&E staining of the retina showed atrophic alterations and disorganized retinal structure at the area of the subretinal channel utilized *eight* times for multiple implantation and explantation procedures. **D** *Localized* lack of rhodopsin staining at the area of the implantation channel is evident (right), *whereas* positive immunohistochemical staining for rhodopsin is observed just outside the channel (left).

Discussion

All our surgeries, eight implantations and eight explantations, were performed as planned without any major complications. The implants could be placed subretinally and stayed at the intended position for the entire examination period in each case. Only one retinal perforation occurred during implant surgery (rabbit 1), an encouraging low rate in light of previously reported series.[25] However, even in this last case the implant could be placed safely in the subretinal space. Neither retinal detachment, nor implant movements, nor any proliferative vitreoretinal alterations over the implant were observed, but in one case retinal atrophy over the implant was seen (rabbit 4). The conjunctival, scleral, and choroidal entry sites were repeatedly usable throughout all surgical procedures and did not show marked signs of atrophy, dehiscence, or infection that would interfere with surgery. As was to be expected, however, repeated surgery required some additional care because of scarring, located mainly within the conjunctiva and connected tissues around the implant material. The operation sites nevertheless always presented with tissue circumstances that allowed safe surgery.

Degeneration of the RPE was observed in rabbits 1 and 2 in the area of the implant 4 weeks after surgery, and also in rabbit 3 where the implant had been left subretinally for 13 months. After subretinal electrical stimulation in rabbit 3, light microscopy showed edema and small degrees of retinal reorganization (Fig. 7A); however, immunohistochemical staining showed intact rhodopsin distribution (Fig. 7B). In rabbit 4 in the area of repeated long-term implantation (approximately after 10 months and eight surgical procedures) the neurosensory retina was disorganized with fibrous tissue formation (Fig. 7C) and defective rhodopsin staining (Fig. 7D, right). However, immediately next to the implantation channel intact rod photoreceptors were found

Jpn J Ophthalmol
Vol 54: 467–475, 2010

(Fig. 7D, left), which allowed successful electrical stimulation. In no case did we observe any cell proliferation—especially not in any Müller cells—between the device and overlying neurosensory retina or between the device and the underlying RPE, reported in other studies.[27,28] Several factors can account for this, such as the different animal species, the different surgical procedures (in our case without an intraocular procedure), and the differences in the coating and electrode material.

Preserved global retinal function after multiple subretinal implantation and explantation surgery was shown by means of intact full-field VEP and ERG in rabbits 3 and 4. A reduction of 20% in the ERG b-wave amplitude does not seem significant considering the typical repeatability and interindividual variability of ERGs. However, it could point to local retinal destruction in the area of the implant, since blockage of nutrient exchange with the RPE inescapably damages the parvangiotic retina in rabbits. VEP recordings showed similar waveforms and amplitudes in the implanted and the unimplanted eye as described before.[24,29]

Intact retinal susceptibility to electrical stimulation after multiple implantation and explantation procedures—even after up to 13 months—was shown by the positive cERG in rabbits 3 and 4, where a clear positive deflection at approximately 20 ms was seen (Fig. 6B). The cERG (Fig. 6B) did not resemble the ERG response to the light flash in terms of shape and implicit time. However, we believe it reflects a biological retinal response evoked by electrical stimulation since it was obtained both before and after pharmacological blockage of the optic nerve by alcohol, but was completely extinguished after the animal was euthanized. cERGS are inherently difficult to record because the temporal proximity of stimulus application and a recording site such that the large stimulus artifacts heavily interfere with the much smaller biological signals. The response time course in rabbits 3 and 4 was slower than that observed in vitro,[20] where the retinal ganglion cell response consisted of a single burst with an implicit time of approximately 13 ms. Implicit time was shorter than for full-field light stimulation, which is in accordance with previous reports for subretinal[19,24] and epiretinal implants,[30] where the authors postulate that electrical stimulation surpasses the relatively slow phototransduction cascade. The discrepancy in shape between the recordings following light and electrical stimulation can possibly be attributed to differences in the characteristics of the input energy and stimulus intensities and to the different retinal cell populations excited.

Intact visual pathway function in terms of susceptibility to electrical stimulation was shown in rabbit 3 by a positive component of the eECP culminating between 10 and 20 ms (Fig. 6A). The response to flash stimuli appeared between 30 and 70 ms. The time difference in response to these different stimuli can again be readily attributed to the bypass of the time-consuming phototransduction cascade by electrical stimulation. Amplitudes of the eECPs were much smaller than those of VEPs, probably because of the size of the stimulated area: with full-field flash stimuli the entire retina is stimulated simultaneously (approximately 1000 mm^2), but the electrodes on the tip of the foil had an area of less than 0.06 mm^2. Unlike in rabbit 3, no discernible response was obtained following electrical stimulation of the eye in rabbit 4, although global retinal function was well preserved as shown by full-field light ERG and VEP (Fig. 5). Considering that the success rate of detecting eECP in our previous experiments in rabbits[24] was 70% (seven of ten eyes), other factors that affected ocular function could be responsible: the particular localization of the electrodes under the retina and their projection to the visual cortex, the position of the recording electrodes over the cortex, or the influence of anesthetics. An alternative explanation could be that previous surgery led to retinal degenerative processes that hindered electrical stimulation. A major factor here is that the rabbit retina is parvangiotic, that is, it depends mostly on diffusion of nutrients from the RPE and not on retinal vessels. Blockage of this diffusion mechanism inevitably leads to degenerative processes in the retina and might damage the nerve fibers in more central areas around the visual streak, thereby leaving the local retinal response intact but disrupting the conduction of any signals via ganglion cell (GC) fibers to the optic nerve. We were able to interrupt transduction of signals through the optic nerve to the brain (electrically or visually evoked) by retrobulbar alcohol injection, sparing retinal responses. The extinction of signals after blockage or transection of the optic nerve (Fig. 6A, B) shows that the responses observed upon electrical stimulation resemble biological responses. In contrast, the positive fast initial responses near 0 ms (Fig. 6) do not reflect physiological responses, first because they appeared immediately after stimulation onset around 0 ms, which is too early for a physiologic response, second, because these responses showed a too-high frequency, and third, because they were present after optic nerve block and euthanizing the animal.

Several drawbacks of our study must be acknowledged. First, the rabbit is certainly not the ideal animal in terms of retinal anatomy since its retina is parvangiotic, which makes it prone to more severe retinal degeneration than animals (such as humans) with holoangiotic retinas, where at least the inner retina is nourished by proprietary retinal vessels and should remain intact even in the presence of a subretinal implant (e.g., Gekeler et al.[31,32]). Second, the number of animals in our study was very small, and each animal was treated differently, which does inhibit statistical analysis. However, we chose rabbits because they are readily available and the surgery procedure is well established, especially the transchoroidal part.[19,24] Further experiments should also make use of modern clinical equipment such as high-resolution optical coherence tomography. Nevertheless, we believe that our findings can constitute a basis for future experiments and hope that they are a stimulus for and promote ongoing discussions regarding human trials.

In summary, our principal finding that repeated transchoroidal surgery for subretinal implants can be safely performed without significant complications and that function in these eyes is maintained demonstrates the feasibility of the transchoroidal approach for implantation, explantation, and reimplantation of retinal prostheses. We believe that

this result will contribute to discussions concerning long-term human trials, when the explantation or exchange of an implant must be dealt with, such as when adverse events occur (e.g., endophthalmitis or retinal detachment), when the device is malfunctioning, or when more advanced implants become available and are demanded by patients. Since several groups are currently using a transchoroidal/transscleral access to the vitreous cavity or the subretinal space[12,17,23] we hope our findings are relevant for subretinally as well as epiretinally placed implants.

Acknowledgments. Support of this study was provided by Uehara Memorial Foundation, the Alexander von Humboldt Foundation and the German Federal Ministry of Education and Research (BMBF), grant 01KP0008. The authors thank Professors Yoshihisa Oguchi and Hisao Ohde for their technical assistance. We gratefully acknowledge the help of our project partners to this work (Institute for Microelectronics, Stuttgart; Institute for Physical Electronics, Stuttgart; Natural and Medical Sciences Institute, Reutlingen; Fraunhofer-Institute for Biomedical Techniques, St. Ingbert; all Germany). Regina Hofer provided the graphics for Fig. 1.

References

1. Chow AY. Electrical stimulation of the rabbit retina with subretinal electrodes and high density microphotodiode array implants. Invest Ophthalmol Vis Sci 1993;34: ARVO Abstract 835.
2. Zrenner E, Miliczek KD, Gabel VP, et al. The development of subretinal microphotodiodes for replacement of degenerated photoreceptors [see comments]. Ophthalmic Res 1997;29:269–280.
3. Yamauchi Y, Franco LM, Jackson DJ, et al. Comparison of electrically evoked cortical potential thresholds generated with subretinal or suprachoroidal placement of a microelectrode array in the rabbit. J Neural Eng 2005;2:48–56.
4. Eckmiller R. Learning retina implants with epiretinal contacts. Ophthalmic Res 1997;29:281–289.
5. Humayun MS, de Juan E, Jr. Artificial vision. Eye 1998;12: 605–607.
6. Humayun MS, de Juan E Jr, Weiland JD, et al. Pattern electrical stimulation of the human retina. Vision Res 1999;39:2569–2576.
7. Rizzo JF, Miller S, Denison T, Herndon T, Wyatt J. Electrically-evoked cortical potentials from stimulation of rabbit retina with a microfabricated electrode array. Invest Ophthalmol Vis Sci 1995;37: ARVO Abstract 707.
8. Rizzo JF, III, Wyatt J, Humayun M, et al. Retinal prosthesis: an encouraging first decade with major challenges ahead. Ophthalmology 2001;108:13–14.
9. Walter P, Heimann K. Evoked cortical potentials after electrical stimulation of the inner retina in rabbits. Graefes Arch Clin Exp Ophthalmol 2000;238:315–318.
10. Kanda H, Morimoto T, Fujikado T, et al. Electrophysiological studies of the feasibility of suprachoroidal–transretinal stimulation for artificial vision in normal and RCS rats. Invest Ophthalmol Vis Sci 2004;45:560–566.
11. Humayun MS, de Juan E Jr, Dagnelie G, et al. Visual perception elicited by electrical stimulation of retina in blind humans. Arch Ophthalmol 1996;114:40–46.
12. Yanai D, Weiland JD, Mahadevappa M, et al. Visual performance using a retinal prosthesis in three subjects with retinitis pigmentosa. Am J Ophthalmol 2007;143:820–827.
13. Caspi A, Dorn JD, McClure KH, et al. Feasibility study of a retinal prosthesis: spatial vision with a 16-electrode implant. Arch Ophthalmol 2009;127:398–401.
14. Chow AY, Chow VY, Packo KH, et al. The artificial silicon retina microchip for the treatment of vision loss from retinitis pigmentosa. Arch Ophthalmol 2004;122:460–469.
15. Roessler G, Laube T, Brockmann C, et al. Implantation and explantation of a wireless epiretinal retina implant device: observations during the EPIRET3 prospective clinical trial. Invest Ophthalmol Vis Sci 2009;50:3003–3008.
16. Zeitz O, Keseru M, Hornig R, Richard G. Artificial sight: recent developments [in German]. Klin Monbl Augenheilkd 2009;226: 149–153.
17. Besch D, Sachs H, Szurman P, et al. Extraocular surgery for implantation of an active subretinal visual prosthesis with external connections: feasibility and outcome in seven patients. Br J Ophthalmol 2008;92:1361–1368.
18. Zrenner E, Wilke R, Bartz-Schmidt K, et al. Blind retinitis pigmentosa patients can read letters and recognize the direction of fine stripe patterns with subretinal electronic implants. Invest Ophthalmol Vis Sci 2009;50: E-Abstract 4581.
19. Chow AY, Chow VY. Subretinal electrical stimulation of the rabbit retina. Neurosci Lett 1997;225:13–16.
20. Stett A, Barth W, Weiss S, et al. Electrical multisite stimulation of the isolated chicken retina. Vision Res 2000;40:1785–1795.
21. Stett A, Kohler K, Weiss S, Haemmerle H, Zrenner E. Electrical stimulation of degenerated retina of RCS rats by distally applied spatial voltage patterns. Invest Ophthalmol Vis Sci 1998;39: ARVO abstract.
22. Stett A, Tepfenhart M, Kohler K, Nuesslin F, Haemmerle H, Zrenner E. Charge sensitivity of electrically stimulated chicken and RCS rat retinae. Invest Ophthalmol Vis Sci 1999;40: ARVO abstract 734.
23. Rizzo JF III, Chen J, Shire D, et al. Implantation of a wirelessly powered retinal prosthesis using an ab externo surgical technique. Invest Ophthalmol Vis Sci 2008; E-Abstract 3027.
24. Gekeler F, Kobuch K, Schwahn HN, Stett A, Shinoda K, Zrenner E. Subretinal electrical stimulation of the rabbit retina with acutely implanted electrode arrays. Graefes Arch Clin Exp Ophthalmol 2004;242:587–596.
25. Shinoda K, Kobuch K, Gekeler F, et al. Transchoroidal implantation of subretinal devices in rabbit: overview of experimental experiences. Invest Ophthalmol Vis Sci 2004 45: E-Abstract 4172.
26. Volker M, Shinoda K, Sachs H, et al. In vivo assessment of subretinally implanted microphotodiode arrays in cats by optical coherence tomography and fluorescein angiography. Graefes Arch Clin Exp Ophthalmol 2004;242:792–799.
27. Kohler KL, Sachs H, Zrenner E, Richter H. Tissue reaction and biocompatibility following long-term implantation of electrical devices into the subretinal space of cats and pigs. Invest Ophthalmol Vis Sci 2003;44: E-Abstract 5071.
28. Loewenstein JI, Rizzo JF, Montezuma SR. Implantation of subretinal polyimide in Yucatan pigs. Invest Ophthalmol Vis Sci 2002 43: E-Abstract 4459.
29. Gekeler F, Schwahn HN, Stett A, Kohler K, Zrenner E. Subretinal microphotodiodes to replace photoreceptor function—a review of the current state. Vision, Sensations et Environnement 2001; 12:77–95.
30. Rizzo JF, Loewenstein J, Wyatt JL, Hollyfield JG, Anderson RE, LaVail MM. Development of an epiretinal electronic visual prosthesis: the Harvard Medical School–Massachusetts Institute of Technology Research Program. Retin Degener Dis Exp Ther 1999;Section IV.463–469.
31. Gekeler F, Szurman P, Grisanti S, et al. Compound subretinal prostheses with extra-ocular parts designed for human trials: successful long-term implantation in pigs. Graefes Arch Clin Exp Ophthalmol 2007 Feb;245:230–241.
32. Gekeler F, Gmeiner H, Volker M, et al. Assessment of the posterior segment of the cat eye by optical coherence tomography (OCT). Vet Ophthalmol 2007;10:173–178.
33. Nadig MN. Development of a silicon retinal implant: cortical evoked potentials following focal stimulation of the rabbit retina with light and electricity. Clin Neurophysiol 1999;110:1545–1553.
34. Sachs HG, Schanze T, Brunner U, Sailer H, Wiesenack C. Transscleral implantation and neurophysiological testing of subretinal polyimide film electrodes in the domestic pig in visual prosthesis development. J Neural Eng 2005;2:S57–S64.

Hindawi Publishing Corporation
Journal of Ophthalmology
Volume 2011, Article ID 564131, 11 pages
doi:10.1155/2011/564131

Clinical Study

Comparison of Photopic Negative Response of Full-Field and Focal Electroretinograms in Detecting Glaucomatous Eyes

Shigeki Machida, Kunifusa Tamada, Taku Oikawa, Yasutaka Gotoh, Tomoharu Nishimura, Muneyoshi Kaneko, and Daijiro Kurosaka

Department of Ophthalmology, School of Medicine, Iwate Medical University, 19-1 Uchimaru Morioka, Iwate 020-8505, Japan

Correspondence should be addressed to Shigeki Machida, smachida@iwate-med.ac.jp

Received 29 April 2010; Revised 24 June 2010; Accepted 22 August 2010

Academic Editor: Christopher Leung

Purpose. To compare the photopic negative response (PhNR) of the full-field electroretinogram (ERG) to the PhNR of the focal ERGs in detecting glaucoma. *Methods.* One hundred and three eyes with glaucoma and 42 normal eyes were studied. Full-field ERGs were elicited by red stimuli on a blue background. The focal ERGs were elicited by a 15° white stimulus spot centered on the macula, the superotemporal or the inferotemporal areas of the macula. *Results.* In early glaucoma, the areas under the receiver operating characteristic curves (AUCs) were significantly larger for the focal PhNR (0.863–0.924) than those for the full-field PhNR (0.666–0.748) ($P < .05$). The sensitivity was significantly higher for the focal PhNR than for the full-field PhNR in early ($P < .01$) and intermediate glaucoma ($P < .05$). In advanced glaucoma, there was no difference in the AUCs and sensitivities between the focal and full-field PhNRs. *Conclusions.* The focal ERG has the diagnostic ability with higher sensitivity in detecting early and intermediate glaucoma than the full-field ERG.

1. Introduction

It has been generally believed that the activity of retinal ganglion cells (RGCs) contributes little to shaping the corneal electroretinogram (ERG) elicited by ganzfeld stimuli (full-field ERG). However, a response has been newly identified to originate from RGCs that receive signals from cones [1]. This response was termed the photopic negative response (PhNR) [2], and it consists of a negative-going wave that follows the photopic cone b-wave.

The PhNR is strongly attenuated in primate's eyes with experimentally induced glaucoma and also in eyes intravitreally injected with tetrodotoxin [2], a blocker of the neural activity of retinal ganglion cells, their axons, and amacrine cells [3, 4]. In addition to this experimental evidence, it has been demonstrated that the PhNR was reduced in patients with optic nerve and retinal diseases that affect mainly the RGCs and retinal nerve fiber layer [5–16]. We have shown that the amplitudes of the PhNR of the full-field cone ERG (full-field PhNR) were correlated with visual sensitivity, disc topography, and retinal nerve fiber layer thickness in eyes with open angle glaucoma (OAG) [16]. These results indicate that the full-field PhNR can be used as an objective functional measure of the RGCs in glaucomatous eyes.

When the full-field PhNR amplitude was used as a diagnostic tool, the sensitivity and specificity to discriminate glaucomatous from normal eyes were 77% and 90%, respectively [16]. However, at the early stage of glaucoma, the sensitivity was reduced to 57%, indicating that the full-field PhNR is not suitable for diagnosing early glaucoma. This is not surprising because the early glaucomatous changes begin with localized neuronal loss in the retina and optic nerve head that could not be detected by the full-field ERG.

The focal ERG system originally developed by Miyake et al. [17] is now commercially available in Japan. Recently, we have recorded focal ERGs from patients with glaucoma [18–20] and optic nerve diseases [21]. We found that the PhNR of the focal ERG (focal PhNR) was also selectively attenuated in patients with OAG. In addition, we investigated

correlation between the focal PhNR and corresponding retinal sensitivity obtained by standard automated perimetry (SAP). A curvilinear relationship was found between the focal PhNR amplitude and retinal sensitivity (decibel), in which a reduction of the focal PhNR amplitude was associated with a small decrease of retinal sensitivity at the early stage of glaucoma [18]. This suggests that the focal PhNR may be used for detecting functional loss at the early stage of glaucoma. This focal ERG system allows us to record focal retinal responses from the paramacular regions of the retina that are preferentially affected at the early stage of glaucoma. In our recent study, we recorded focal ERGs from three retinal loci including the macular region, the supero-temporal and infero-temporal areas of the macula. The sensitivity and specificity of the focal PhNR to discriminate early glaucoma were >90%. These findings were made with the combined criterion in which eyes were classified as being glaucomatous when the focal PhNR amplitudes were less than the optimal cut-off values in either retinal locus [19].

From these results, it appeared that the focal PhNR is better than the full-field PhNR to discriminate glaucomatous from normal eyes. However, a direct comparative study comparing the diagnostic values of full-field and focal PhNRs obtained from the same eyes has not been reported although studies using different patient populations for the full-field and focal PhNRs have been done [16, 18, 19].

Thus, the purpose of this study was to compare the ability of the full-field and focal PhNRs to detect glaucomatous eyes at different stages. Importantly, the full-field and focal PhNRs were recorded from the same eyes.

2. Methods

2.1. Patients. One hundred and three eyes of 103 patients with OAG were studied. Their ages ranged from 37 to 83 years with a mean ± standard deviation of 68.2 ± 9.1 years. The diagnosis of OAG was based on the presence of a glaucomatous optic disc associated with visual field defects measured by SAP. The presence of glaucomatous optic disc was determined by the guideline of Japanese Society of Glaucoma developed in 2005 (http://www.nichigan.or.jp/member/guideline/glaucoma2.jsp). According to the diagnostic criterion for minimal abnormality of the visual field [22], the visual field defect was determined to be glaucomatous when it met one of three criteria. (1) The pattern deviation plot showed a cluster of three or more nonedge points that had lower sensitivities than those in 5% of the normal population ($P < .05$), and one of the points had a sensitivity that was lower than 1% of the population ($P < .01$), (2) the value of the corrected pattern standard deviation was lower than that of 5% of the normal visual field ($P < .05$), or (3) the Glaucoma Hemifield Test showed that the field was outside the normal limits.

Forty-two eyes of 42 age-matched normal volunteers, ranging in age from 53 to 78 years with a mean of 67.6 ± 7.3 years, were studied. We selected normal eyes from patients with macular hole in the fellow eye which was treated by vitrectomy. They underwent comprehensive ophthalmological examinations including measuring visual acuity by a Snellen chart and observing the ocular fundus by an indirect ophthalmoscope as well as a biomicroscopic slit lamp. In addition, we performed optical coherence tomography and SAP to rule out macular and optic nerve diseases.

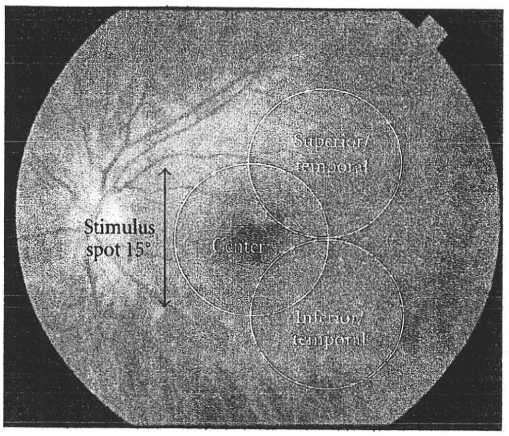

FIGURE 1: Ocular fundus photograph showing retinal areas which were stimulated by focal spots with a diameter of 15 degrees.

This research was conducted in accordance with the Institutional Guidelines of Iwate Medical University, and the procedures conformed to the tenets of the Declaration of Helsinki. An informed consent was obtained from all subjects after a full explanation of the nature of the experiments.

2.2. ERG Recordings. The pupils were maximally dilated to approximately 8 mm in diameter following topical application of a mixture of 0.5% tropicamide and 0.5% phenylephrine HCL. The recordings of the full-field and focal ERGs were made on the same eye on the same day. The stimulus conditions for the recordings of the full-field cone ERGs and focal ERGs have been reported in detail [16, 18].

The full-field cone ERGs were elicited by red stimuli of 1 600 cd/m^2 (λ_{max} = 644 nm, half-amplitude bandwidth = 35 nm) on a blue background of 40 cd/m^2 (λ_{max} = 470 nm, half-amplitude bandwidth = 18 nm). The duration of the stimulus was 3 msec. The stimulus and background lights were produced by light emitting diodes (LEDs) embedded in the contact lens.

Focal ERGs were recorded from the macular area and from the supero-temporal and infero-temporal areas of the macula. Responses from these areas are designated as the center, superior/temporal, and inferior/temporal responses, respectively (Figure 1). The stimulus system was integrated into the infrared fundus camera (Mayo Co., Nagoya, Japan), which had been developed by Miyake et al. [17]. The stimulus spot was 15 degrees in diameter and was placed on the retinal area of interest, and the position was confirmed by viewing the ocular fundus on a monitor. The intensity of the white stimulus and background lights was 165 cd/m^2 and 6.9 cd/m^2, respectively. The stimulus duration was 10 ms. The focal ERGs were recorded with a Burian-Allen bipolar

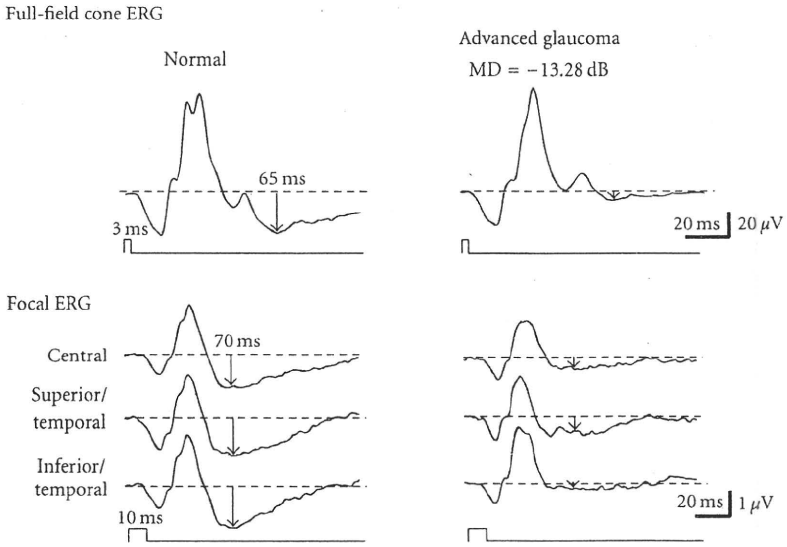

FIGURE 2: Representative full-field cone and focal electroretinograms recorded from a normal subject and a glaucoma patient with advanced visual field defects.

contact lens electrode (Hansen Ophthalmic Laboratories, Iowa City, IA).

The responses were digitally band-pass filtered from 0.5 to 1000 Hz for the full-field ERG and from 5 to 500 Hz for the focal ERG. It is often difficult to determine the negative trough of the PhNR especially in cases with reduced PhNR amplitudes. Therefore, we measured the PhNR amplitude at the fixed time points. We determined the time of the maximum amplitude of the PhNR in normal subjects according to the method of Rangaswamy et al. [9]. We found that the full-field and focal PhNRs were the largest at 65 ms and 70 ms after the flash, respectively. Therefore, we measured PhNR amplitudes at 65 ms for the full-field PhNR and 70 ms for the focal PhNR throughout the study (Figure 2).

2.3. Visual Field Analyses. The Humphrey Visual Field Analyzer (Model 750, Humphrey Instruments, San Leandro, CA, USA) was used for SAP. The SITA Standard strategy was applied to program 24-2. From the mean deviation (MD) of the 24-2 program, we classified patients with glaucomatous visual fields into three groups: early (MD > -6 dB; $n = 41$, mean age and SD: 68.6 ± 9.8 years), intermediate (-6 dB $\geq$ MD ≥ -12 dB; $n = 28$, 69.5 ± 8.1 years), and advanced (MD < -12 dB; $n = 34$, 69.4 ± 7.4 years) defects of the visual field. There was no significant difference in the mean age among the three groups. The intraocular pressures (IOPs) of all patients were controlled under 21 mmHg by eye drops, and there was no significant difference in the IOPs among the groups. The averaged MDs were -3.31 ± 1.58, -8.88 ± 1.67, and -17.37 ± 4.46 dB for the early, intermediate, and advanced groups, respectively.

When the fixation loss rate is higher than 20%, the field examination was determined to be unreliable and excluded from the analysis. In addition, when the false-positive or false-negative error rates exceeded 33%, the visual field was not used for the analysis. The interval between the visual field testing and ERG recording was less than 1 month.

2.4. Statistic Analyses. We used receiver operating characteristic (ROC) curves to determine the optimal cut-off values that yielded the highest likelihood ratio. The area under the curve (AUC) was used to compare the ROC curves. The comparison between AUCs was made according to the method reported by DeLong et al. [23]. The sensitivity and specificity of the focal PhNR were compared to that of the PhNR of the full-field ERGs using Fisher's exact test. Unpaired t tests were used to compare data between groups with different degrees of the visual field defect. One-way ANOVA was used to determine the statistical significance of the ERG changes in eyes with the stage of glaucoma. These analyses were performed using commercial software MedCalc 11.3.3 (MedCalc Software, Mariakerke, Belgium) and Prism 5.1 (GraphPad Software Inc., San Diego, CA).

3. Results

3.1. Representative ERG Waveforms from Normal and Glaucomatous Eyes. The full-field and focal ERGs recorded from a normal control and a patient that had advanced glaucoma with a mean deviation -13.28 dB are shown in Figure 2. Both the full-field and focal PhNRs were reduced in the patient compared to the normal control although there was no change in the amplitudes of the a- and b-waves in the full-field and focal ERGs (Figure 2).

3.2. Averaged PhNR Amplitudes and PhNR/b-Wave Amplitude Ratios for Different Degrees of Visual Field Defects. We have plotted the PhNR amplitudes and PhNR/b-wave amplitude

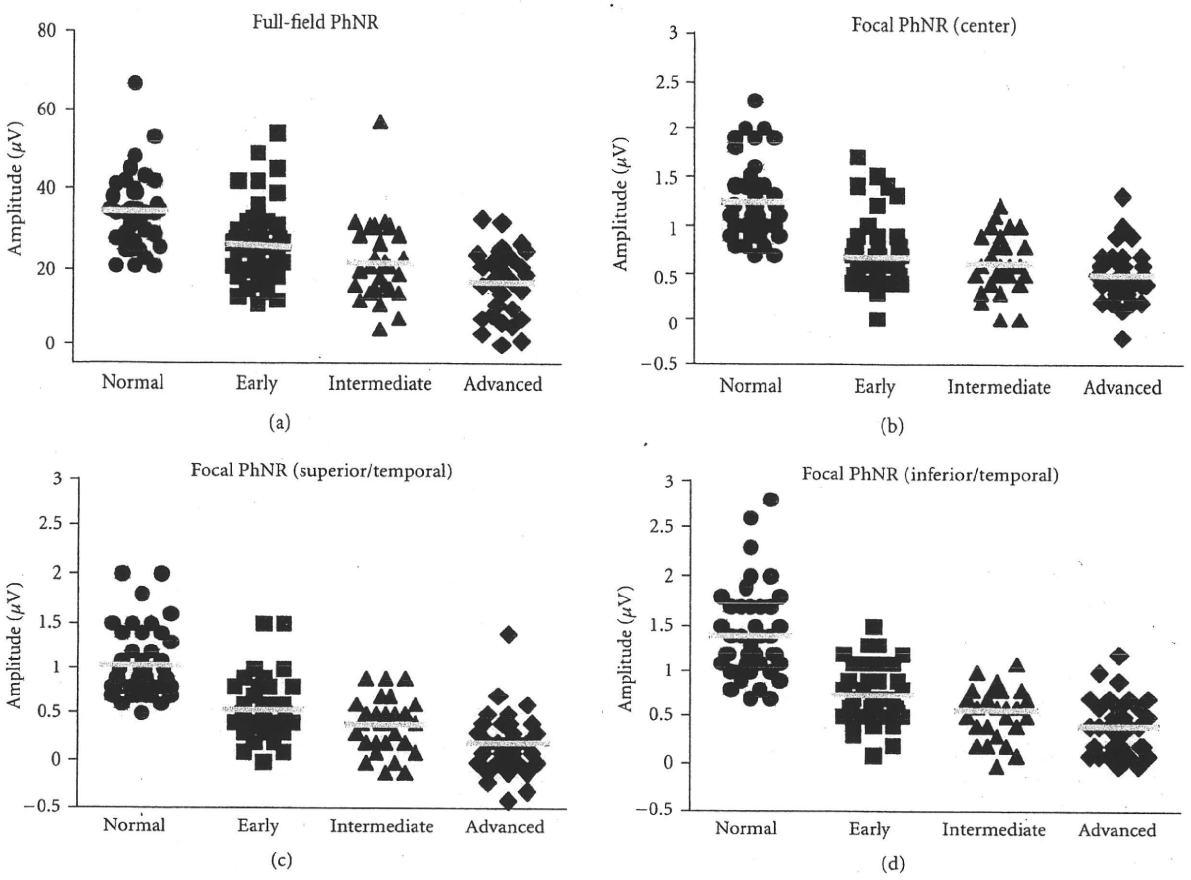

FIGURE 3: The PhNR amplitudes of the full-field (a) and focal ERGs (b) center, (c) superior/temporal, and (d) inferior/temporal) are plotted for the normal controls (●) and glaucomatous eyes at early (■), intermediate (▲), and advanced stages (♦). Bars represent means of the PhNR amplitudes.

ratios against stages of glaucoma in Figures 3 and 4, respectively. In both the full-field and focal ERGs, the PhNR amplitudes and the PhNR/b-wave amplitude ratios were significantly and progressively reduced with an advance in the stage of glaucoma ($P < .0001$). Even at the early stage of glaucoma, the PhNR amplitude and PhNR/b-wave amplitude ratio were significantly reduced compared to that in the normal controls for the full-field (PhNR amplitude: $P < .004$) and focal ERGs (all retinal areas: $P < .0001$). However, for the PhNR/b-wave amplitude ratio of the full-field ERGs, the data of the normal control considerably overlapped those from the early glaucoma group resulting in no significant differences (Figure 4(a)).

The PhNR amplitude and PhNR/b-wave amplitude ratio of the full-field ERGs gradually decreased as the stage of glaucoma advanced. On the other hand, the greatest loss of the PhNR amplitude and PhNR/b-wave amplitude ratio of the focal ERG was seen at the early stage of glaucoma. For example, the mean of the focal PhNR amplitude recorded from the center was reduced from 1.24 μV to 0.69 μV at the early stage of glaucoma. Then, it slightly decreased to 0.50 μV at the advanced stage of glaucoma despite considerable loss of the visual sensitivity of SAP (Figure 3(b)).

The full-field PhNR amplitude fell outside the normal range in 29, 48, and 56% of patients of the early, intermediate, and advanced groups. The focal PhNR amplitudes of the central retinal area fell outside the normal range in 62, 61, and 76% of patients of the early, intermediate and advanced groups. The corresponding percentages for the superior/temporal and inferior/temporal focal PhNR amplitudes were 49 and 46% for the early, 59 and 57% for the intermediate, and 85 and 79% for the advanced groups, respectively. Thus, the focal PhNR amplitude showed abnormal values in more patients at any stages than the full-field PhNR amplitude. Similar results were obtained for the PhNR/b-wave amplitude ratio.

3.3. ROC Curves of Full-Field and Focal ERGs. The cut-off values were varied by 1.0 μV steps for the full-field PhNR amplitude, 0.1 μV for the focal PhNR amplitudes, and 0.01 for the focal PhNR/b-wave amplitude ratio for the pooled data of glaucomatous and normal eyes. The sensitivity and specificity were obtained for each cut-off value and plotted to determine the ROC curves from which the AUC was obtained (Figures 5–7, Table 1).

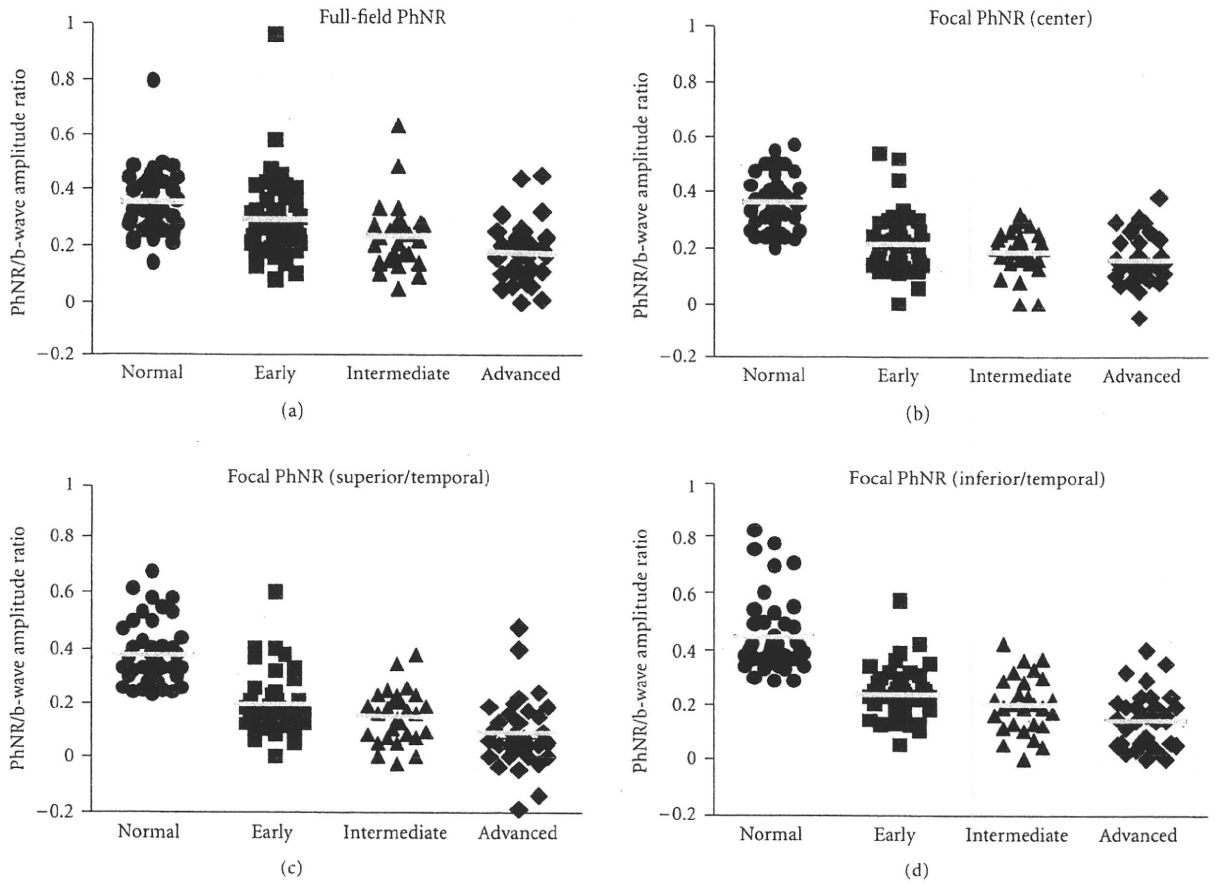

FIGURE 4: The PhNR/b-wave amplitude ratios of the full-field (a) and focal ERGs (b) center, (c) superior/temporal, and (d) inferior/temporal) are plotted for the normal controls (●) and glaucomatous eyes at early (■), intermediate (▲), and advanced stages (♦). Bars represent means of the PhNR/b-wave amplitude ratios.

In early glaucoma, the focal PhNR amplitude curves were always superior to the full-field PhNR amplitude curves. As a result, the AUC of the focal PhNR amplitude of the inferior/temporal area was significantly larger than that of the full-field PhNR amplitude (Figure 5(a), $P < .05$). The AUCs of the focal PhNR/b-wave amplitude ratio obtained from all retinal areas were significantly larger than those of the full-field PhNR/b-wave amplitude ratio (Figure 5(b), Table 1, $P = .01$ for the center, $P = .001$ for the superior/temporal area, and $P < .001$ for the inferior/temporal area).

For eyes with intermediate glaucoma, most parts of the ROC curves of the focal ERG amplitudes overlapped the curve of the PhNR amplitude of the full-field ERGs. Thus, there was no significant difference in the AUCs between the focal and full-field PhNR amplitudes (Figure 6(a)). For the PhNR/b-wave amplitude ratio, the curves of the focal PhNR/b-wave amplitude ratio were always higher than those of the full-field PhNR/b-wave amplitude ratio, resulting in significantly larger AUCs for the focal PhNR/b-wave amplitude ratio than for the full-field PhNR/b-wave amplitude ratio (Figure 6(b), $P < .05$ for the center, $P < .01$ for the inferior/temporal and superior/temporal areas).

In eyes with advanced glaucoma, the ROC curves for the PhNR amplitude and PhNR/b-wave amplitude ratio of the focal and full-field ERGs were overlapped (Figure 7). The differences in the AUCs between the full-field and focal PhNRs for both the PhNR amplitude and PhNR/b-wave amplitude ratio were not significant.

3.4. Sensitivity and Specificity of Full-Field and Focal ERG PhNR. The sensitivity and specificity were obtained with the optimal cut-off values for the PhNR amplitude (Table 2) and the PhNR/b-wave amplitude ratio (Table 3). Because the likelihood ratio reveals the sensitivity/false positive rate, the highest likelihood ratio indicates high sensitivity and specificity. Eyes were classified as being glaucomatous when their focal PhNR amplitudes or focal PhNR/b-wave amplitude ratio were less than the cut-off values in either retinal areas (combined criterion in Tables 2 and 3). In all patient groups with different degrees of visual field defects, no significant difference was found in the specificity between the full-field and focal PhNRs obtained from all retinal areas including the combined criteria.

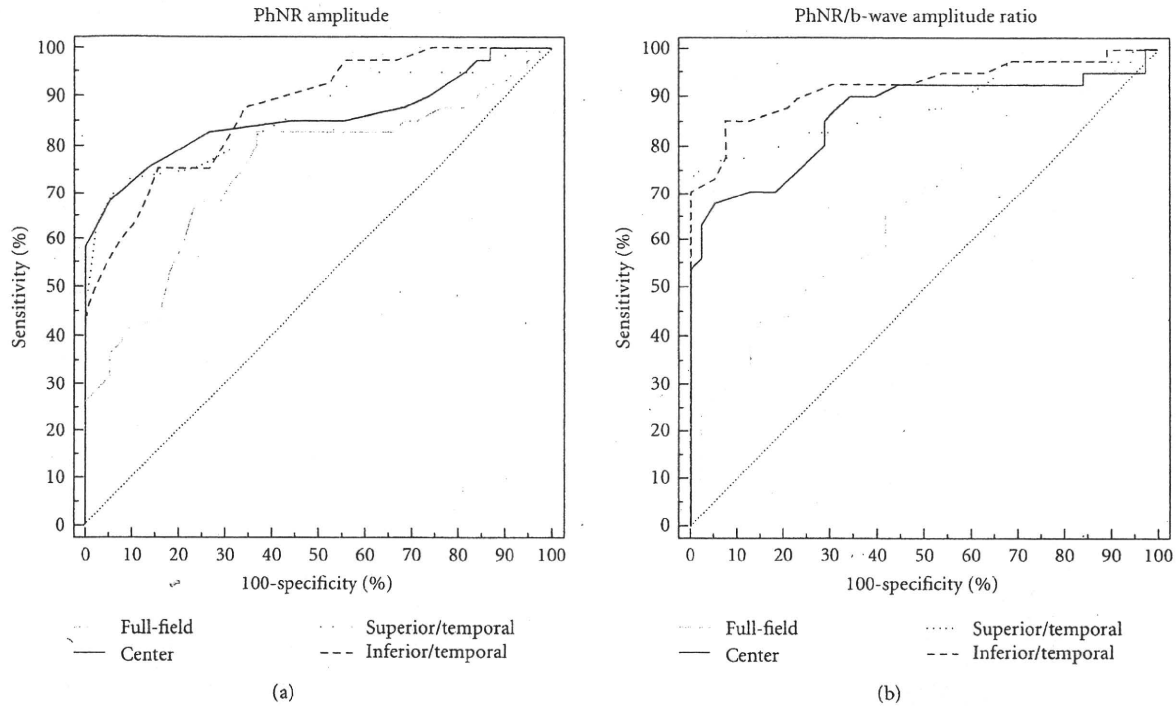

FIGURE 5: Receiver operating characteristic (ROC) curves for the PhNR amplitude (a) and PhNR/b-wave amplitude ratio (b) of the full-field and focal electroretinograms. Patients with early glaucoma ($n = 41$, mean deviation > -6 dB). PhNR: photopic negative response.

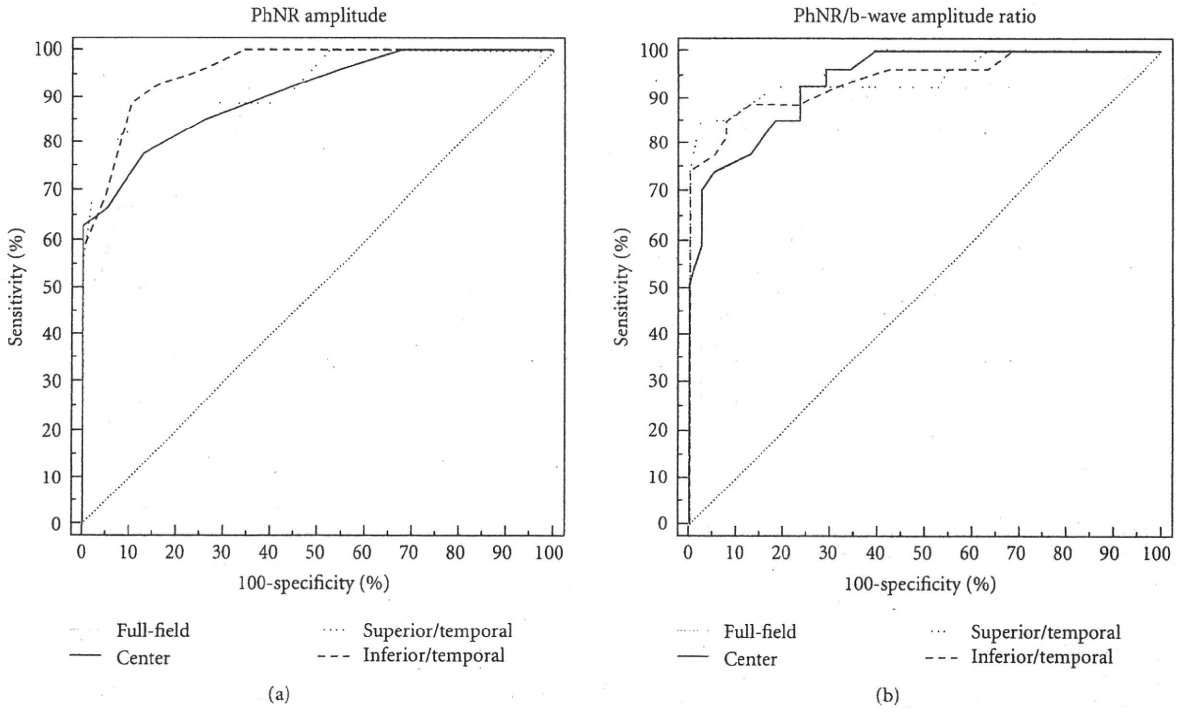

FIGURE 6: Receiver operating characteristic (ROC) curves for the PhNR amplitude (a) and PhNR/b-wave amplitude ratio (b) of the full-field and focal electroretinograms. Patients with intermediate glaucoma ($n = 28$, -6 dB $\geq$ mean deviation ≥ -12 dB). PhNR: photopic negative response.

Table 1: Area under the curve of the PhNR amplitude and PhNR/b-wave amplitude ratio.

	PhNR amplitude		PhNR/b-wave amplitude ratio	
	AUC	95% CI	AUC	95% CI
Early (n = 41)				
Full-field ERG	0.748	0.638–0.839	0.666	0.551–0.768
Focal ERG				
Center	0.866	0.759–0.925	0.863	0.767–0.930
Sup/temp	0.863	0.767–0.930	0.886	0.795–0.947
Inf/temp	0.874	0.780–0.938	0.924	0.841–0.971
Intermediate (n = 28)				
Full-field ERG	0.865	0.758–0.937	0.789	0.670–0.880
Focal ERG				
Center	0.906	0.808–0.964	0.938	0.849–0.982
Sup/temp	0.929	0.838–0.978	0.946	0.860–0.987
Inf/temp	0.959	0.878–0.992	0.942	0.854–0.984
Advanced (n = 34)				
Full-field ERG	0.954	0.875–0.989	0.910	0.817–0.965
Focal ERG				
Center	0.951	0.871–0.988	0.930	0.842–0.977
Sup/temp	0.968	0.895–0.995	0.953	0.874–0.989
Inf/temp	0.972	0.902–0.996	0.972	0.901–0.996

PhNR: photopic negative response; AUC: area under the curve; CI: confidence interval; sup/temp: superior/temporal; inf/temp: inferior/temporal.

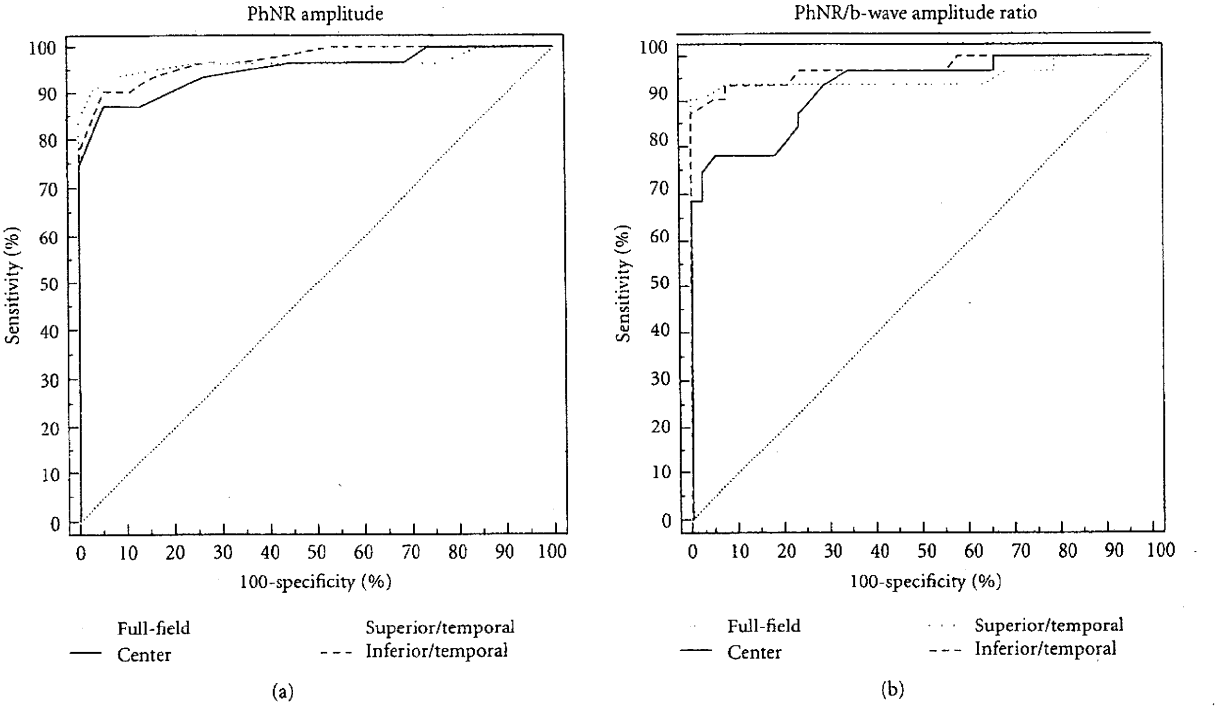

Figure 7: Receiver operating characteristic (ROC) curves for the PhNR amplitude (a) and PhNR/b-wave amplitude ratio (b) of the full-field and focal electroretinograms. Patients with *advanced* glaucoma (n = 34, mean deviation < −12 dB). PhNR: photopic negative response.

Table 2: Sensitivity and specificity of the PhNR amplitude to discriminate glaucomatous eyes.

	Sensitivity (95%CI)	Specificity (95%CI)	Cut-off value (μV)
Early ($n = 41$)			
Full-field ERG	38.1 (23.6–54.4)	92.3 (79.1–98.3)	22
Focal ERG			
Center	69.1 (52.9–82.4)	95.2 (83.8–99.3)	0.7
Sup/temp	63.4 (46.9–77.9)	97.6 (87.1–99.6)	0.5
Inf/temp	56.1 (46.9–77.9)	95.2 (83.8–99.3)	0.7
Combined	88.1 (74.4–96.0)	90.5 (87.7–99.6)	
Intermediate ($n = 28$)			
Full-field ERG	59.3 (38.8–77.6)	92.3 (79.1–98.3)	22
Focal ERG			
Center	64.3 (44.1–81.3)	95.2 (83.8–99.3)	0.7
Sup/temp	75.0 (55.1–89.3)	97.6 (87.1–99.6)	0.5
Inf/temp	67.9 (47.7–84.1)	95.2 (83.8–99.3)	0.7
Combined	92.9 (87.7–99.6)	90.5 (87.7–99.6)	
Advanced ($n = 34$)			
Full-field ERG	66.7 (48.2–82.0)	92.3 (79.1–98.3)	22
Focal ERG			
Center	88.2 (72.5–96.6)	95.2 (83.8–99.3)	0.7
Sup/temp	90.9 (75.6–98.0)	97.6 (87.1–99.6)	0.5
Inf/temp	90.9 (75.6–98.0)	95.2 (83.8–99.3)	0.7
Combined	97.1 (87.7–99.6)	90.5 (87.7–99.6)	

PhNR: photopic negative response; CI: confidence interval; sup/temp: superior/temporal; inf/temp: inferior/temporal.

Table 3: Sensitivity and specificity of the PhNR/b-wave amplitude ratio to discriminate glaucomatous eyes.

	Sensitivity (95%CI)	Specificity (95%CI)	Cut-off value
Early ($n = 41$)			
Full-field ERG	23.8 (12.1–39.5)	97.4 (86.5–99.6)	0.19
Focal ERG			
Center	61.9 (45.6–76.4)	97.6 (87.4–99.6)	0.22
Sup/temp	75.6 (59.7–87.6)	97.6 (87.1–99.6)	0.23
Inf/temp	73.1 (57.1–85.3)	95.2 (83.8–99.3)	0.29
Combined	97.6 (87.7–99.6)	92.9 (87.7–99.6)	
Intermediate ($n = 28$)			
Full-field ERG	40.7 (22.4–61.2)	97.4 (86.5–99.6)	0.20
Focal ERG			
Center	67.9 (47.7–84.1)	97.6 (87.4–99.6)	0.22
Sup/temp	85.7 (67.3–95.9)	97.6 (87.1–99.6)	0.23
Inf/temp	78.6 (59.0–91.7)	95.2 (83.8–99.3)	0.29
Combined	96.4 (87.7–99.6)	92.9 (87.7–99.6)	
Advanced ($n = 34$)			
Full-field ERG	69.7 (51.3–84.4)	97.4 (86.5–99.6)	0.20
Focal ERG			
Center	70.6 (52.5–84.9)	97.6 (87.4–99.6)	0.22
Sup/temp	90.9 (75.6–98.0)	95.6 (87.1–99.6)	0.23
Inf/temp	90.9 (75.6–98.0)	95.2 (83.8–99.3)	0.29
Combined	97.1 (87.7–99.6)	92.9 (87.7–99.6)	

PhNR: photopic negative response; CI: confidence interval; sup/temp: superior/temporal; inf/temp: inferior/temporal.

In patients with mild defects of the visual field, the sensitivities of the focal PhNR amplitudes were significantly higher than those of the full-field PhNR amplitudes ($P < .01$) except for the inferior/temporal area. For the PhNR/b-wave amplitude ratio, the sensitivities of the focal ERG in both retinal areas were significantly higher than those of the full-field ERGs ($P < .001$ for the center, $P < .00001$ for the superior/temporal and inferior/temporal areas). The sensitivities of the PhNR amplitude and PhNR/b-wave amplitude ratio increased to 88.1% and 97.6%, respectively, when the combined criterion was used, and they were significantly higher than the corresponding values of the full-field PhNR ($P < .00001$).

In intermediate and advanced glaucoma, the sensitivities of the focal PhNRs were generally higher than those of the full-field PhNRs. A significant difference was found between the focal and full-field PhNRs in the PhNR/b-wave amplitude ratio obtained from the superior/temporal and inferior/temporal areas in intermediate glaucoma ($P < .01$ for the superior/temporal retinal area, $P < .05$ for the inferior/temporal area). The sensitivities of the focal PhNR obtained by the combined criteria were significantly higher than those of the full-field PhNR in intermediate glaucoma ($P < .05$ for the PhNR amplitude, $P < .005$ for the PhNR/b-wave amplitude ratio).

In advanced glaucoma, there was no significant difference in the sensitivity between the full-field and focal PhNRs.

4. Discussion

We compared diagnostic abilities between the full-field and focal PhNRs in detecting glaucomatous eyes. Our results demonstrated that the AUCs and sensitivities were higher for the focal PhNR than for the full-field PhNR at the early and intermediate stages of glaucoma. This suggests that the focal PhNR is a good indicator to detect the functional loss in early and intermediate glaucoma.

4.1. Diagnostic Ability of Full-Field and Focal PhNRs. The AUCs of the focal PhNRs were better for identifying eyes with early and intermediate glaucoma than those of the full-field PhNRs. On the other hand, there was no significant difference in the AUCs between the focal and full-field PhNRs in advanced glaucoma. When the combined criterion for the focal PhNR was used, the sensitivity increased to 88.1% and 97.6% for the focal PhNR amplitude and PhNR/b-wave amplitude ratio, respectively, even in early glaucoma, while the sensitivities for the PhNR amplitude and amplitude ratio of the full-field ERG were 38.1% and 23.8%. These findings indicate that the focal PhNR is a better indicator than the full-field PhNR in detecting functional changes in early and intermediate glaucoma.

We selected the optimal cut-off value with the highest likelihood ratio which maximally reduces false positive cases. This then kept the specificity high for both PhNR parameters. The disadvantage of the combined criterion is that it lowers the specificity as reported although a high sensitivity was obtained [18]. However, the specificity of the PhNR of the full-field and focal ERGs could be kept over 90% by using this method to select the optimal cut-off values. Our results indicated that, even in early glaucoma, the focal PhNR had high sensitivity and specificity attained by the combined criterion.

We have reported that a curvilinear relationship existed between the retinal sensitivity (in decibels) measured by perimetry and the focal PhNR amplitude [18]. This indicated that 3 dB loss in the retinal sensitivity is approximately associated with a fifty percent decrease in the focal PhNR amplitude at the early stage of glaucoma. In fact, the largest loss of the PhNR amplitude was seen at the early stage of glaucoma in the focal ERGs (Figures 3 and 4). On the other hand, the full-field PhNR amplitude gradually reduced with advance of glaucoma. Taken together, these findings indicate that the focal PhNR could be a better measure to detect functional abnormalities at the early stage of glaucoma than the full-field PhNR.

4.2. Disadvantages of Focal PhNR. It is essential that the ocular fundus is visible to be able to record the focal PhNRs reliably because the stimulus areas stimulated must be monitored during the recordings using an infrared fundus camera. It is impossible to record the focal ERG in patients with dense opacities of the ocular media, such as cataracts and vitreous opacities. Furthermore, opacities of the ocular media can produce stray-light that makes the focal stimulus larger. Therefore, we have excluded patients with clinically significant cataracts that affected vision. On the other hand, the stray-light effect is negligible for the full-field ERGs. In cases with severe opacity of the ocular media, the full-field PhNRs would be more reliable than the focal PhNR.

Intersession variability is represented by the coefficients of variation (CV = standard deviation/mean $\times$ 100), and it was higher for the focal PhNR than for the full-field PhNR [16, 18]. In addition, variations of the PhNR amplitude among individuals were greater for the focal PhNR amplitude than for the full-field PhNR amplitude [18]. However, this disadvantage of the focal PhNR can be reduced by using the amplitude ratio of the PhNR to the b-wave amplitude [18]. Therefore, the PhNR/b-wave amplitude ratio is recommended for measuring the effectiveness of the focal ERGs.

4.3. Limitations of the Present Study. The recording and stimulus conditions of the focal ERG were different from those of full-field ERG, which may explain why the focal PhNR was better than the full-field PhNR in diagnosing early or intermediate glaucoma. First, we set the low cut filters at 0.5 Hz and 5 Hz for the full-field and focal ERGs, respectively. The higher cut-off frequency (5 Hz) used to record the focal PhNR was necessary to eliminate the drifts in the baseline. Thus, some of the low frequency components of the PhNR were reduced as shown in monkeys [24, 25].

Second, the full-field ERGs were elicited by red stimuli on a blue background (R/B) while the focal ERGs were elicited by white stimuli on a white background (W/W). The R/B stimuli have been shown to be a very good combination to

elicit large and reliable PhNRs [26]. Furthermore, the results of our preliminary study demonstrated that the sensitivity and specificity to discriminate glaucoma were higher for the R/B than for the W/W stimulus conditions (Machida et al., *IOVS* 2007; 48: ARVO E-Abstract 215). Thus, the stimulus conditions used in this study are more advantageous to eliciting full-field PhNRs than focal PhNRs.

Therefore, the differences in the recording and stimulus conditions do not seem to be able to explain the current results in which the focal PhNR was more sensitive than the full-field PhNR in diagnosing early and intermediate glaucoma.

5. Conclusions

The results of this study indicate that the PhNRs of the full-field and focal ERGs represent functional loss of RGCs in glaucoma at different stages of glaucoma. The focal ERG has the diagnostic ability with high sensitivity and specificity in detecting glaucomatous eyes at the early and intermediate stages, especially when the combined criterion is used. There was no difference in the diagnostic value between the full-field and focal PhNRs in advanced glaucoma. Thus, the focal PhNR can be a good functional parameter to detect early or intermediate glaucoma.

Acknowledgments

This paper was supported by a Grant-in-Aid for Scientific Research C from Ministry of Education, Science, and Culture in Japan no. 20592056, Grant from Keiryokai Research Foundation no. 102, grant from The Imai Memorial Fund for Research.

References

[1] W. Spileers, F. Falcao-Reis, R. Smith, C. Hogg, and G. B. Arden, "The human ERG evoked by a ganzfeld stimulator powered by red and green light emitting diodes," *Clinical Vision Sciences*, vol. 8, no. 1, pp. 21–39, 1993.

[2] S. Viswanathan, L. J. Frishman, J. G. Robson, R. S. Harwerth, and E. L. Smith III, "The photopic negative response of the macaque electroretinogram: reduction by experimental glaucoma," *Investigative Ophthalmology and Visual Science*, vol. 40, no. 6, pp. 1124–1136, 1999.

[3] T. Narahashi, "Chemicals as tools in the study of excitable membranes," *Physiological Reviews*, vol. 54, no. 4, pp. 813–889, 1974.

[4] S. A. Bloomfield, "Effect of spike blockade on the receptive-field size of amacrine and ganglion cells in the rabbit retina," *Journal of Neurophysiology*, vol. 75, no. 5, pp. 1878–1893, 1996.

[5] A. Colotto, B. Falsini, T. Salgarello, G. Iarossi, M. E. Galan, and L. Scullica, "Photopic negative response of the human ERG: losses associated with glaucomatous damage," *Investigative Ophthalmology and Visual Science*, vol. 41, no. 8, pp. 2205–2211, 2000.

[6] S. Viswanathan, L. J. Frishman, J. G. Robson, and J. W. Walters, "The photopic negative response of the flash electroretinogram in primary open angle glaucoma," *Investigative Ophthalmology and Visual Science*, vol. 42, no. 2, pp. 514–522, 2001.

[7] N. Drasdo, Y. H. Aldebasi, Z. Chiti, K. E. Mortlock, J. E. Morgan, and R. V. North, "The S-cone PhNR and pattern ERG in primary open angle glaucoma," *Investigative Ophthalmology and Visual Science*, vol. 42, no. 6, pp. 1266–1272, 2001.

[8] Y. Gotoh, S. Machida, and Y. Tazawa, "Selective loss of the photopic negative response in patients with optic nerve atrophy," *Archives of Ophthalmology*, vol. 122, no. 3, pp. 341–346, 2004.

[9] N. V. Rangaswamy, L. J. Frishman, E. U. Dorotheo, et al., "Photopic ERGs in patients with optic neuropathies: comparison with primate ERGs after pharmacological blockade of inner retina," *Investigative Ophthalmology & Visual Science*, vol. 45, pp. 3827–3837, 2004.

[10] S. Machida, Y. Gotoh, M. Tanaka, and Y. Tazawa, "Predominant loss of the photopic negative response in central retinal artery occlusion," *American Journal of Ophthalmology*, vol. 137, no. 5, pp. 938–940, 2004.

[11] J. Kizawa, S. Machida, T. Kobayashi, Y. Gotoh, and D. Kurosaka, "Changes of oscillatory potentials and photopic negative response in patients with early diabetic retinopathy," *Japanese Journal of Ophthalmology*, vol. 50, no. 4, pp. 367–373, 2006.

[12] S. Ueno, M. Kondo, C.-H. Piao, K. Ikenoya, Y. Miyake, and H. Terasaki, "Selective amplitude reduction of the PhNR after macular hole surgery: ganglion cell damage related to ICG-assisted ILM peeling and gas tamponade," *Investigative Ophthalmology and Visual Science*, vol. 47, no. 8, pp. 3545–3549, 2006.

[13] H. Chen, D. Wu, S. Huang, and H. Yan, "The photopic negative response of the flash electroretinogram in retinal vein occlusion," *Documenta Ophthalmologica*, vol. 113, no. 1, pp. 53–59, 2006.

[14] K. Miyata, M. Nakamura, M. Kondo et al., "Reduction of oscillatory potentials and photopic negative response in patients with autosomal dominant optic atrophy with OPA1 mutations," *Investigative Ophthalmology and Visual Science*, vol. 48, no. 2, pp. 820–824, 2007.

[15] H. Chen, M. Zhang, S. Huang, and D. Wu, "The photopic negative response of flash ERG in nonproliferative diabetic retinopathy," *Documenta Ophthalmologica*, vol. 117, no. 2, pp. 129–135, 2008.

[16] S. Machida, Y. Gotoh, Y. Toba, A. Ohtaki, M. Kaneko, and D. Kurosaka, "Correlation between photopic negative response and retinal nerve fiber layer thickness and optic disc topography in glaucomatous eyes," *Investigative Ophthalmology and Visual Science*, vol. 49, no. 5, pp. 2201–2207, 2008.

[17] Y. Miyake, K. Yanagida, K. Yagasaki, et al., "Subjective scotometry and recording of local electroretinogram and visual evoked response. System with television monitor of the fundus," *Japanese Journal of Ophthalmology*, vol. 25, no. 4, pp. 438–448, 1981.

[18] S. Machida, Y. Toba, A. Ohtaki, Y. Gotoh, M. Kaneko, and D. Kurosaka, "Photopic negative response of focal electoretinograms in glaucomatous eyes," *Investigative Ophthalmology & Visual Science*, vol. 49, no. 12, pp. 5636–5644, 2008.

[19] S. Machida, K. Tamada, T. Oikawa, et al., "Sensitivity and specificity of photopic negative response of focal electroretinograms in detecting glaucomatous eyes," *British Journal of Ophthalmology*, vol. 94, pp. 202–208, 2010.

[20] K. Tamada, S. Machida, T. Oikawa, et al., "Correlation between photopic negative response of focal electroretinograms and local loss of retinal neurons in glaucoma," *Current Eye Research*, vol. 35, pp. 155–164, 2010.

[21] K. Tamada, S. Machida, D. Yokoyama, and D. Kurosaka, "Photopic negative response of full-field and focal electroretinograms in patients with optic nerve atrophy," *Japanese Journal of Ophthalmology*, vol. 53, pp. 608–614, 2009.

[22] D. R. Anderson and V. M. Patella, *Automated Static Perimetry*, Mosby, St. Louis, Mo, USA, 2nd edition, 1999.

[23] E. R. DeLong, D. M. DeLong, and D. L. Clarke-Pearson, "Comparing the areas under two or more correlated receiver operating characteristic curves: a nonparametric approach," *Biometrics*, vol. 44, no. 3, pp. 837–845, 1988.

[24] M. Kondo, Y. Kurimoto, T. Sakai et al., "Recording focal macular photopic negative response (PhNR) from monkeys," *Investigative Ophthalmology and Visual Science*, vol. 49, no. 8, pp. 3544–3550, 2008.

[25] Y. Kurimoto, M. Kondo, S. Ueno, T. Sakai, S. Machida, and H. Terasaki, "Asymmetry of focal macular photopic negative responses (PhNRs) in monkeys," *Experimental Eye Research*, vol. 88, no. 1, pp. 92–98, 2009.

[26] N. V. Rangaswamy, S. Shirato, M. Kaneko, B. I. Digby, J. G. Robson, and L. J. Frishman, "Effects of spectral characteristics of ganzfeld stimuli on the photopic negative response (PhNR) of the ERG," *Investigative Ophthalmology and Visual Science*, vol. 48, no. 10, pp. 4818–4828, 2007.

Jpn J Ophthalmol 2010;54:458–466
DOI 10.1007/s10384-010-0842-9

LABORATORY INVESTIGATION

Pharmacological Dissection of Multifocal Electroretinograms of Rabbits with Pro347Leu Rhodopsin Mutation

Daisuke Yokoyama[1], Shigeki Machida[1], Mineo Kondo[2], Hiroko Terasaki[2], Tomoharu Nishimura[1], and Daijiro Kurosaka[1]

[1] Department of Ophthalmology, Iwate Medical University School of Medicine, Morioka, Iwate, Japan; [2] Department of Ophthalmology, Nagoya University Graduate School of Medicine, Nagoya, Japan

Abstract

Purpose: To determine whether photoreceptor degeneration in transgenic (Tg) rabbits carrying the Pro347Leu *rhodopsin* mutation alters the neural activity of the middle and inner retinal neurons.

Methods: Multifocal electroretinograms (mfERGs) were recorded from eight 12-week-old Tg rabbits both before and after intravitreal injection of the following: tetrodotoxin citrate (TTX), *N*-methyl-DL-aspartic acid (NMDA), 2-amino-4-phosphonobutyric acid (APB), and *cis*-2,3-piperidine-dicarboxylic acid (PDA). Digital subtraction of the mfERGs recorded after the drugs were administered from those recorded before was used to extract the components that were eliminated by these drugs. Eight age-matched, wild-type (WT) rabbits were studied with the same protocol.

Results: There was no reduction in the amplitude of the cone photoreceptor response of the mfERGs in Tg rabbits. Both the first positive and the first negative waves of the ON-bipolar cell responses were significantly larger in the Tg than in the WT rabbits. Late negative waves of the ON-bipolar cell response were recorded only in the WT rabbits. The first negative wave of the inner retinal responses was larger in the Tg than in the Wt rabbits. The late positive waves were seen mainly in the WT rabbits.

Conclusions: The ON-bipolar cell and inner retinal responses were altered at the early stage of photoreceptor degeneration in Tg rabbits despite the preservation of the cone photoreceptor responses. **Jpn J Ophthalmol** 2010;54:458–466 © Japanese Ophthalmological Society 2010

Keywords: ERG, multifocal ERG, Pro347Leu, retinitis pigmentosa, rhodopsin mutation

Introduction

More than 100 distinct mutations of the *rhodopsin* gene have been associated with autosomal dominant retinitis pigmentosa (adRP) (http://www.sph.uth.tmc.edu/RetNet/). Among these, mutations involving the carboxy terminus of the *rhodopsin* gene, such as Pro347Leu, are associated with poor visual outcomes.[1,2] The development of animal models with mutations found in retinitis pigmentosa (RP) patients is very important for understanding the pathophysiology of RP and for developing new treatments for RP. Mice, rats, and pigs with mutations of the carboxy terminus of the *rhodopsin* gene have been developed, and their retinal morphology and physiology have been studied.[3–5] More recently, Kondo et al.[6] created transgenic (Tg) rabbits with the Pro347Leu *rhodopsin* mutation, and these rabbits showed a progressive loss of photoreceptors. They used electroretinography to assess the physiology of the retina of wild-type (WT) and Tg rabbits, and demonstrated that the loss of rod function precedes that of the cones in Pro347Leu *rhodopsin* Tg rabbits.[6] Interestingly, the oscillatory potentials (OPs) of the cone electroretinograms (ERGs) were larger in the young Tg rabbits than in the WT rabbits.[7] Pharmacological analysis has shown that an intravitreal injection of tetrodo-

Received: October 28, 2009 / Accepted: March 29, 2010
Correspondence and reprint requests to: Shigeki Machida, Department of Ophthalmology, Iwate Medical University School of Medicine, 19-1 Uchimaru, Morioka, Iwate 020-8505, Japan
e-mail: smachida@iwate-med.ac.jp

toxin (TTX), which blocks the sodium channels of the retinal ganglion and amacrine cells,[8–10] eliminates the enhanced OPs in the young Tg rabbits.[7] This indicates that the inner retinal responses are altered at the early stage of photoreceptor degeneration in the Tg rabbits.

Histopathological analyses have demonstrated that photoreceptors are altered predominantly in the posterior pole of the fundus rather than in the peripheral region of the retina.[6] This indicates that the early functional changes take place in the posterior pole of the retina in Tg rabbits. Multifocal ERGs (mfERGs) consist mainly of responses from the middle and inner retinal layers of the posterior pole of the ocular fundus.[11] Therefore, examination of mfERGs allows us to analyze how the middle and inner retinal functions are affected by photoreceptor degeneration in the posterior pole of the ocular fundus at the early stage. Ng et al.[12] demonstrated that in pigs with photoreceptor degeneration induced by a Pro347Leu *rhodopsin* mutation, the mfERG components from the middle and inner retinal layers are altered.

The purpose of the present study was to determine whether the neural activity of the middle and inner retinal neurons is altered by photoreceptor degeneration in Tg rabbits carrying the Pro347Leu *rhodopsin* mutation. To accomplish this, we recorded mfERGs from Tg rabbits, and used different combinations of drugs to isolate the responses from the outer, middle, and inner retina. We then compared the responses of the Tg rabbits with those of WT rabbits.

Methods

Animals

Heterozygous Pro347Leu *rhodopsin* Tg rabbit line 7, which has the highest level of transgene expression and the most severe photoreceptor degeneration, was used.[6] In these rabbits the transgene copy number estimated by Southern blot analysis was 30, and the ratio of transgene to endogenous opsin mRNA was 4:1. The histopathological and electrophysiological characteristics as well as the natural course of degeneration for line 7 of Tg rabbits had already been documented.[6] Eight 10-week-old Tg rabbits were purchased from Kitayama Labs (Nagano, Japan) and kept in the animal colony until the experiments. Eight WT New Zealand albino rabbits were used as controls. The experiments were performed on all rabbits when they were 12 weeks of age.

All animals were housed and handled under the authorization and supervision of the Institutional Animal Care and Use Committee of Iwate Medical University. All procedures conformed to the ARVO Resolution on the Use of Animals in Ophthalmic and Vision Research.

mfERG Recordings

The rabbits were anesthetized with a loading dose of intramuscular xylazine (2 mg/kg) and ketamine (25 mg/kg), and then maintained under anesthesia by hourly injections of a mixture of xylazine (1 mg/kg) and ketamine (13 mg/kg). The pupils were maximally dilated with a mixture of 0.5% tropicamide and 0.5% phenylephrine HCL applied topically.

Before the recordings, the rabbits were light-adapted for at least 15 min in a room with an ambient illumination of 252 lux. The refractive error was measured with a refractometer (Retinomax K-plus 2, Nikon, Tokyo, Japan). The average spherical equivalent of the refractive error was +3.9 ± 0.9 diopters (D) for the WT and 3.8 ± 1.2 D for the Tg rabbits. Therefore, +4.0 D (for the refractive error) and +3.0 D (for the testing distance) lenses were placed in front of the tested eyes.

The Visual Evoked Response Imaging System (VERIS, Mayo, Nagoya, Japan) was used to record the mfERGs. Stimuli were generated on a 17-inch (about 43 cm) Cathode Ray Tube (CRT) monitor and consisted of 61 equal-sized hexagonal elements. Both white (200 cd/m^2) and black (4 cd/m^2) elements were presented in a pseudorandom binary m-sequence at a stimulus frequency of 75 Hz. A steady background of 100 cd/m^2 surrounded the stimulus field.

The location of the optic nerve heads were approximated by indirect ophthalmoscopy, and the body and head of the animal were adjusted so that the optic axis was directed to the center of the stimulus field. The CRT monitor was placed 30 cm from the cornea and subtended at a visual angle of 50° horizontally and 40° vertically.

Initially, mfERGs were recorded and the eye position was adjusted until the amplitudes from the visual streaks were larger than those recorded from the surrounding areas and the mfERGs from areas corresponding to the optic disc were smaller than those recorded from the surrounding areas. These recorded waveforms were designated as the baseline mfERGs.

The responses were band-pass filtered from 10 to 300 Hz and amplified (Model 12 A5C, Astro-Med, West Warwick, RI, USA). VERIS software (VERIS Science 4.0, Mayo) was used for the mfERG analyses, and the all-trace waveforms of the first-order kernels were obtained by averaging the local retinal responses from the 61 different retinal loci. The amplitudes of the all-trace waveforms are expressed as response density (nV/deg^2) representing the amplitude/stimulus area.

Drug Administration

Tetrodotoxin citrate (TTX; Latoxan, Valence, France), *N*-methyl-DL-aspartic acid (NMDA), 2-amino-4-phosphonobutyric acid (APB), or *cis*-2,3-piperidine-dicarboxylic acid (PDA) (all from Sigma, St. Louis, MO, USA) were injected into the vitreous cavity of each Tg and Wt rabbit to isolate the responses driven by the photoreceptors, bipolar cells, and third-order neurons, including the retinal ganglion and amacrine cells. The retinal responses driven by bipolar cells and the third-order neurons were defined as